PHYSICS

R. M. S. Joemai
J. Geleijns
W. J. H. Veldkamp

Development and validation of a low dose simulator for computed tomography

R. M. S. Joemai · J. Geleijns ·
W. J. H. Veldkamp
Radiology Department, Leiden
University Medical Centre,
Albinusdreef 2,
2333 ZA, Leiden, The Netherlands

R. M. S. Joemai (✉)
Radiology Department, Leiden
University Medical Centre,
PO Box 9600,
2300 RC, Leiden, The Netherlands
e-mail: R.M.S.Joemai@lumc.nl
Tel.: +31-71-5263687
Fax: +31-71-5248256

Abstract *Purpose:* To develop and validate software for facilitating observer studies on the effect of radiation exposure on the diagnostic value of computed tomography (CT). *Methods:* A low dose simulator was developed which adds noise to the raw CT data. For validation two phantoms were used: a cylindrical test object and an anthropomorphic phantom. Images of both were acquired at different dose levels by changing the tube current of the acquisition (500 mA to 20 mA in five steps). Additionally, low dose simulations were performed from 500 mA downwards to 20 mA in the same steps. Noise was measured within the cylindrical test object and in the anthropomorphic phantom. Finally, noise power spectra (NPS) were measured in water. *Results:* The low dose simulator yielded similar image quality compared with actual low dose acquisitions. Mean difference in noise over all comparisons between actual and simulated images was $5.7 \pm 4.6\%$ for the cylindrical test object and $3.3 \pm 2.6\%$ for the anthropomorphic phantom. NPS measurements showed that the general shape and intensity are similar. *Conclusion:* The developed low dose simulator creates images that accurately represent the image quality of acquisitions at lower dose levels and is suitable for application in clinical studies.

Keywords Computed tomography · X-ray · Radiation · Physics · Computer simulation · Noise

Introduction

Computed tomography (CT) imaging plays a prominent role in the diagnosis and follow-up of patients with the introduction of multislice, dual source and volumetric CT. CT is increasingly used for a growing variety of signs and symptoms and CT examinations are associated with relatively high radiation exposure to patients. In developed countries, radiation dose from medical diagnostic radiology constitutes about 20–50% of the collective dose with a substantial contribution of CT [1]. Patients benefit from well-justified referrals for diagnostic radiology examinations. However growing concern exists about the possible occurrence of late stochastic effects (carcinogenesis) resulting from radiation exposure to patients [2]. Conse-

quently, there is growing interest in the optimisation of CT acquisition protocols.

The parameter that mainly determines patient exposure for well-defined clinical CT acquisitions is the effective tube charge (effective mAs). Tube charge is proportional to patient exposure but it is also closely related to image quality, particularly to the contrast-to-noise ratio in the reconstructed images. Noise is in general expressed as the standard deviation of Hounsfield units (HU). If research showed that appropriate diagnosis were achievable with CT images that contain relatively higher noise levels, this would mean that dose reduction would be feasible; for example, allowing image noise to increase by a factor of 2 would imply that a dose reduction by a factor of 4 would be achieved.

Exploring the feasibility of dose reduction in clinical CT can be done in appropriately designed clinical studies and was first described by Mayo et al. [3]. Whereas imaging of volunteers for optimisation of acquisition protocols in magnetic resonance imaging is common practice, studies on the effect of tube charge on CT image quality cannot be performed on volunteers. Legislation and ethical considerations do not allow such practices in CT as it would require multiple exposures of the volunteers. Therefore, there is great interest in the development and application of a low dose CT simulator that adds noise to clinical CT and that yields studies mimicking image quality of low dose CT acquisitions.

Development and validation of such a low dose simulator has been described previously for radiography [4] and this approach is now extended to CT. It has been shown that it is possible to simulate exposure reduction by adding spatially correlated noise to reconstructed images [5]; however, the same research group states that there is no doubt that the ideal method is to add noise to raw projection data. In the current study we used the latter approach, like most other groups that report on low dose simulations in CT [3, 6–10]. This paper reports on the development and validation of the low dose CT simulator that is applied to raw data of CT acquisitions. Low dose simulations and actual acquired low dose images of a cylindrical test object and an anthropomorphic phantom were compared to quantitatively assess the performance of the simulation tool.

Materials and methods

Acquisition and reconstruction protocol

Imaging was performed on an Aquilion 64 CT (Toshiba Medical Systems, Otawara, Japan; software version 4.10). Calibration data were acquired to determine the relation between raw data pixel value and noise. This was achieved using homogeneous cylindrical water-filled calibration objects that had the same diameter as the imaging field of view (FOV). From five available FOVs (500, 400, 320, 240 and 180 mm) the three most frequently used FOVs were chosen for this evaluation, i.e. 400, 320 and 240 mm. For each combination of tube voltage and FOV, calibration CT data were acquired (360° acquisition without table feed) using 64×0.5-mm beam collimation and 0.5-s rotation time. Tube currents were 500, 300, 150, 80, 40, 20 and 10 mA. The calibration data were derived directly from the raw data; therefore no image reconstructions were made from these acquisitions.

Evaluation of image quality and validation of the low dose CT simulator were performed using two phantoms: a cylindrical test object with various inserts, corresponding HU are approximately −1,000 HU, 320 HU, 120 HU, 90 HU, −110 HU, 0 HU (CT performance phantom,

Toshiba Medical Systems), and an anthropomorphic phantom representing a trunk and head of an average sized male (Rando phantom, manufactured in one piece, The Phantom Laboratory, New York, USA). The following configurations were used for imaging the test object and anthropomorphic phantom: 64×0.5 mm (number of active detector rows × detector row width), rotation time 0.5 s and pitch factor 0.823. Acquisitions were performed at a tube voltage of 120 kV and tube currents of 500, 300, 150, 80, 40 and 20 mA, respectively. These six acquisitions were performed for three FOVs of 400, 320 and 240 mm. Images were reconstructed at 1.0-mm slice thickness and a 1.0-mm reconstruction interval; the reconstruction kernel was FC12 (soft). No additional software filters were used for noise suppression or artefact reduction.

Algorithm of the low dose CT simulator

A low dose CT simulator was developed in MATLAB (MATLAB R2007b, The MathWorks Inc, Novi, MI, USA). The application can be run standalone on every PC and creates CT raw data representing lower dose CT acquisitions.

General principles were described by Veldkamp et al. [4] for application in digital chest radiography and similar approaches have been described previously [3, 11]. Two preconditions need to be met for proper application of the method mentioned above. First, raw data values need to be transformed to become linear with the dose at the detector. To achieve this, a logarithmic operation was applied to the raw data to obtain a linear relation between the raw data pixel value for each detector element and dose. Second, the relationship between the transformed raw data values and their associated noise (expressed as standard deviation) must be established. A calibration procedure establishes this relationship from the raw data acquired from the homogeneous, water-filled calibration objects. The raw data (or sinograms) of the CT are two-dimensional matrices. The columns in the matrix are associated with the position of detector elements along the detector arc; the number of columns thus corresponds with the number of detector elements along the detector arc. The rows in the matrix are associated with the projection angle. Each acquisition at a 64×0.5-mm configuration yields 64 sinograms.

Axial 360° CT was performed for the calibration and was derived from all 64 sinograms, each with 900 projections. For all projections and for each detector element noise and raw data pixel values were measured in the raw data. The mean noise and raw data pixel value were established for each detector element over all projections. This was done for each sinogram separately and the results were averaged over all 64 sinograms and stored as a look-up table (LUT) in a spreadsheet. Accordingly, the LUT contains data representing the relation between noise and raw data pixel value for each detector element. For each

relevant combination of tube voltage (kV) and FOV a separate LUT was determined. Linear interpolation between the measured data or linear extrapolation from these data was applied to determine the desired simulated noise levels for each raw data pixel value for each detector element.

The low dose CT simulator divides raw data pixel values (y) by a dose reduction quotient q which results in new simulated raw data pixel values y/q. Next, both standard deviations, original (σ_y) and desired ($\sigma_{y'}$), are determined from the calculated relation between noise and pixel value in the LUT for each raw data pixel value. The quotient q' is determined between σ_y and $\sigma_{y'}$. Finally, to simulate lower dose images, values from a Gaussian distribution with zero mean and standard deviation σ_G are added to the down-scaled raw image data y/q. It is shown that σ_G must satisfy the following equation to obtain the desired noise level [4]:

$$\sigma_G^2 = \sigma_y^2 \cdot \frac{q^2 - q'^2}{q^2 \cdot q'^2} \tag{1}$$

After addition of noise the transformed raw data are inverse transformed using an inverse logarithmic operation; the resulting sinogram was uploaded to the CT and was reconstructed by the actual reconstructor of the CT.

Evaluation with a cylindrical test object

Noise and HU were measured in six regions of interest (ROI) corresponding to six different materials and averaged over 50 slices of the cylindrical test object. The calculated mean noise and mean HU were recorded. The results of the simulated images were compared with the results of the acquired images at the corresponding dose.

The ROI in water was also used for measurement of the noise power spectrum (NPS). The NPS was calculated as described by Boedeker et al. [12]. In short, the procedure was as follows: the NPS was calculated from the test object images by extracting a centred 128×128 matrix from each slice. Next, the mean pixel value of the extracted matrix was subtracted from the matrix to avoid an offset in the Fourier transform. The extracted matrix was then zero-padded to a 512×512 image to achieve increased resolution. The Fourier transform of each extended matrix was calculated and the square of the magnitude was calculated. Additionally the usual NPS normalisation was performed. Here the normalisation term was obtained by the product of pixel spacing in horizontal and vertical directions divided by the product of image size in horizontal and vertical directions (512×512). To improve accuracy, the result was averaged over all 50 slices and used in the calculation. This approach resulted in a two-dimensional NPS. To present this as a one-dimensional NPS representation with reduced statistical variation, the NPS was radially averaged for each of the acquired 256 frequency bins.

Evaluation with an anthropomorphic phantom

The anthropomorphic phantom was used for validation of the CT low dose simulator by means of noise measurements. The phantom consisted of a skeleton and lung-
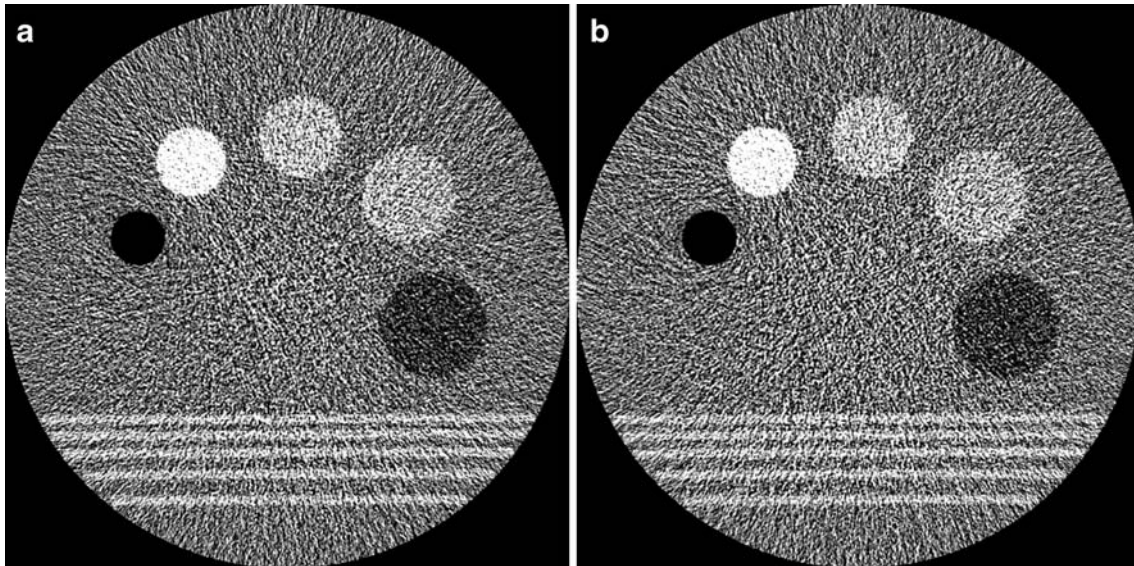

Fig. 1 An acquired image corresponding to 40 mA (**a**) and a simulated image from an acquisition at 500 mA to 40 mA (**b**). The simulated image of the cylindrical test object expresses comparable noise levels and shows a realistic representation (window width/ window level=400/40). The corresponding tube voltage and FOV are 120 kV and 320 mm. The phantom is filled with water and contains five objects with different densities (HU)

tissue-equivalent material, surrounded by soft-tissue-equivalent material [13]. The phantom was imaged over a length of 290 mm including the whole thorax and a part of the abdomen. For the noise measurements, software was developed using MATLAB. The software performed segmentation of the soft-tissue-like material. Next, for each slice a grid of small, square ROIs was created and the noise was calculated separately for all ROIs that were entirely located in the soft-tissue-like material. The median of the standard deviation values was recorded for each slice. The results of the simulated images were compared with the results of the acquired images at the same dose.

Data analysis

Results of noise and HU measurements in the cylindrical phantom are expressed as mean ± standard deviation. Noise measurements, corresponding to the entire range from shoulders to abdomen in the anthropomorphic phantom, were visualised as box-and-whisker plots. The top and bottom of each box represent the 75th and 25th percentile, respectively, while the central line represents the median. The whiskers show the maximum and minimum noise level. Comparisons are all calculated as absolute differences.
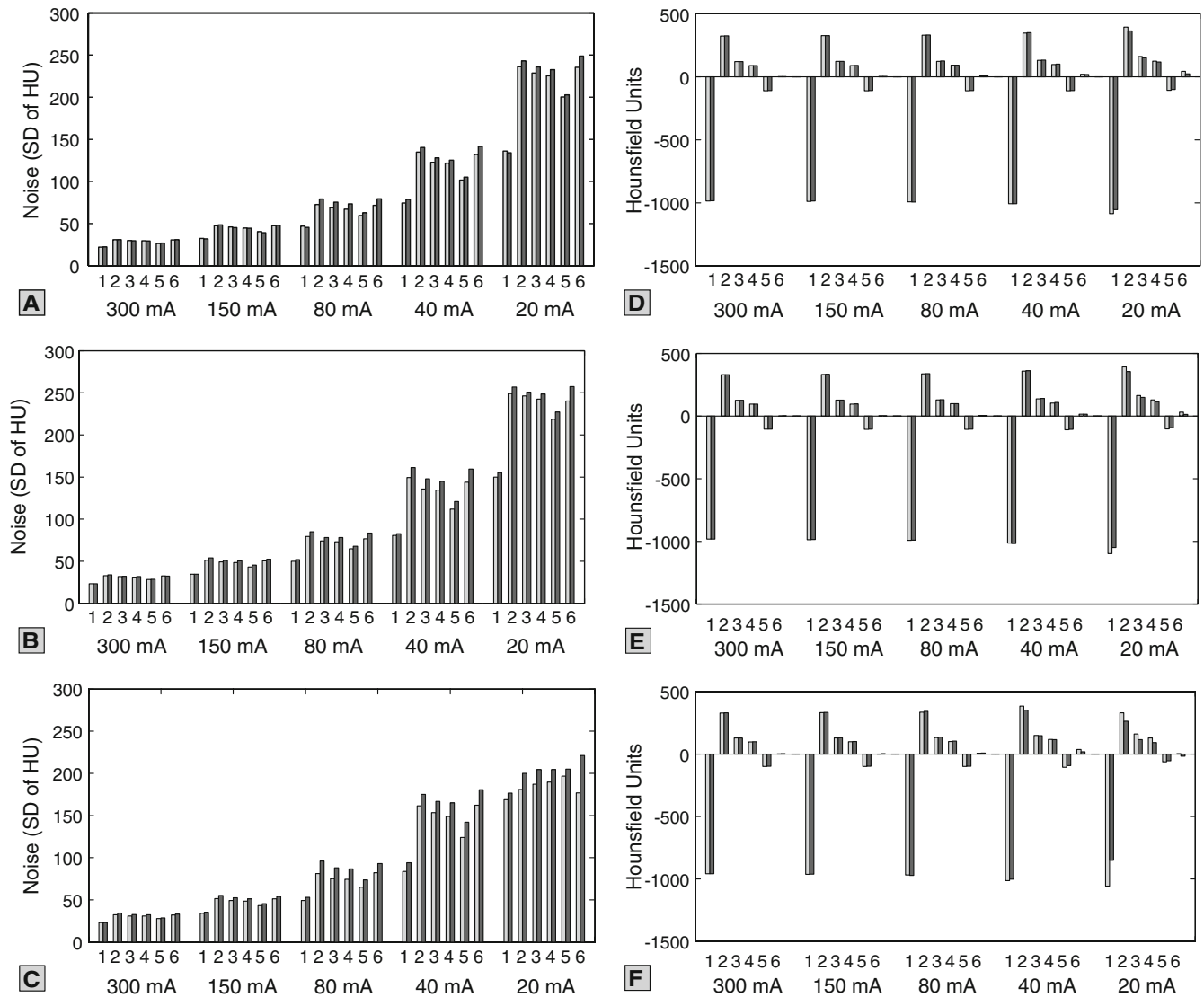

Fig. 2 Noise (**a**–**c**) and Hounsfield units (HU) (**d**–**f**) measurements in acquired and simulated images of the cylindrical test object. Simulations were performed from 500 mA downwards to 300, 150, 80, 40 and 20 mA. The measurements are performed in six ROIs.

Light bars indicate acquired and *dark bars* simulated images. Three configurations were evaluated: 120 kV in combination with FOV 400 mm (**a**, **d**), FOV 320 mm (**b**, **f**), FOV 240 mm (**c**, **e**). *HU* Hounsfield unit, *SD* standard deviation

Results

Cylindrical test object

Visual inspection of actual and simulated images of the test object showed good similarities (Fig. 1). In Fig. 2a–c the results of the noise measurements and in Fig. 2d–f the results of the mean HU value measurements are shown. In most comparisons, a slight overestimation of noise in simulated images was found. Mean differences in noise measurements between actual and simulated images were calculated over all slices for six ROIs at five dose levels and three FOVs (Table 1). Evaluations showed larger differences in noise for FOV 240 mm than for 320 mm and smallest differences were calculated for 400 mm. Mean differences in noise per FOV were respectively 9.0±5.4%, 4.5±2.9% and 3.5±3.0%. Mean differences in noise per dose level showed differences within 10%, i.e. 1.9±1.9% (300 mA), 3.8±2.2% (150 mA), 9.4±4.6% (80 mA), 7.8±3.4% (40 mA) and 5.6±5.5% (20 mA). Noise measurements at a dose level of 20 mA and a FOV of 240 mm showed comparable noise levels for the different ROIs, most likely because of the proportionally more prominent effect of detector noise in relation to quantum noise at a low tube current. HU measurements showed good agreement between actual and simulated images. In general, the differences slightly increase with lower dose levels. The NPS results are compared in Fig. 3 for a FOV of 320 mm. The general shape and intensity are similar.
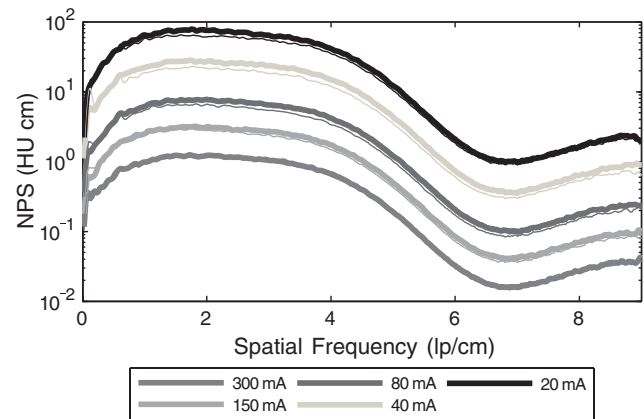

Fig. 3 Noise power spectrum (NPS); *thick lines* are simulated and *thin lines* represent measurements in actual images. The images were acquired with tube voltage 120 kV and FOV 320 mm. Slice thickness was 1.0 mm with a reconstruction interval of 1.0 mm

Anthropomorphic phantom

Visual inspection of actual and simulated images of the anthropomorphic phantom showed good similarities. Images in both the shoulder (sensitive for photon starvation) and the lung area were also similar (Fig. 4).

Figure 5 shows an example of noise profiles for an actual and simulated series (tube voltage 120 kV and FOV 320 mm). The graphs show similar noise levels for the simulated images compared with the actual acquisition

Table 1 Mean differences in noise between actual and simulated images of the cylindrical phantom in six ROIs

|		Differences (%)				
		300 mA	150 mA	80 mA	40 mA	20 mA
120 kV–FOV 400 mm	ROI1	1.05	1.46	2.76	6.06	1.50
	ROI2	0.09	1.93	8.94	4.02	2.85
	ROI3	0.72	1.64	9.17	4.32	3.19
	ROI4	0.14	0.50	9.12	2.96	3.18
	ROI5	1.36	2.63	5.52	3.58	1.29
	ROI6	0.80	1.28	10.90	7.33	5.72
120 kV–FOV 320 mm	ROI1	0.00	0.26	3.94	2.46	3.48
	ROI2	3.28	5.36	6.98	7.86	3.12
	ROI3	0.91	3.73	5.44	8.83	1.81
	ROI4	2.86	4.23	6.95	7.62	2.49
	ROI5	0.72	5.26	4.72	8.01	3.96
	ROI6	0.36	4.35	9.03	10.97	7.13
120 kV–FOV 240 mm	ROI1	0.38	3.40	7.92	12.30	4.61
	ROI2	6.05	7.33	18.25	8.40	10.50
	ROI3	5.63	6.89	16.88	8.83	9.36
	ROI4	4.59	6.19	16.60	10.67	7.82
	ROI5	2.76	5.67	13.07	14.75	4.19
	ROI6	3.04	5.67	13.04	11.24	25.04
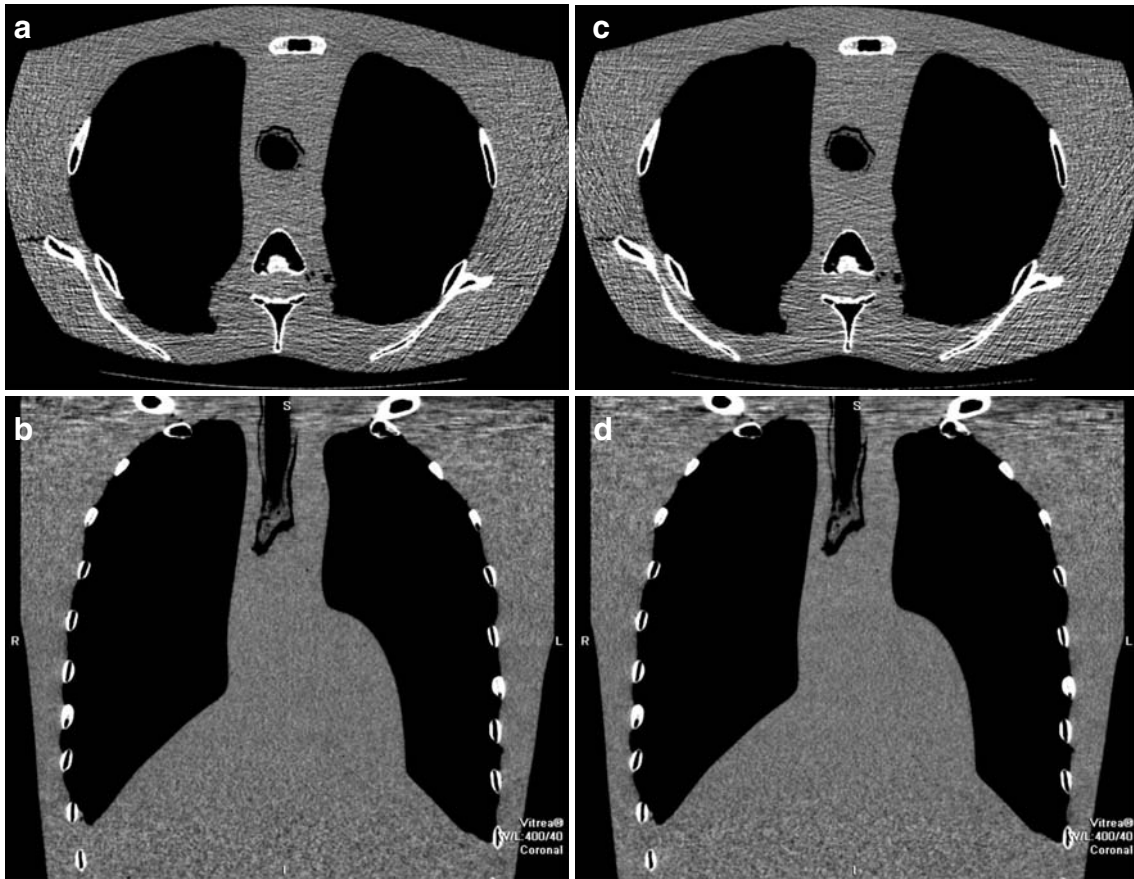
Fig. 4 An acquired image with 40 mA (**a**, **b**) and a simulated image from an acquisition at 500 mA to 40 mA (**c**, **d**). Axial and MPR reconstructions were both performed. The simulated images of the anthropomorphic phantom contain comparable noise levels and show realistic representation (window width/window level= 400/40). The corresponding tube voltage and FOV are 120 kV and 320 mm
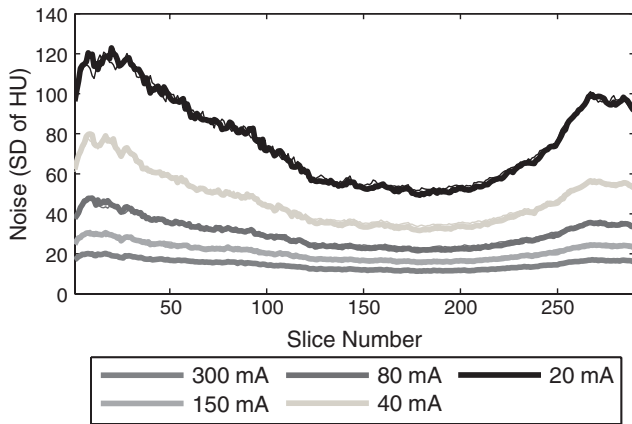

Fig. 5 Example of noise profiles in the anthropomorphic phantom. CT was performed from the shoulders (low slice numbers) to the abdomen (high slice numbers). The noise on the *y*-axis corresponds to the standard deviation of HUs in the soft-tissue-simulating material. The corresponding tube voltage and FOV were 120 kV and 320 mm. Simulations were performed from 500 mA downwards to 300, 150, 80, 40 and 20 mA. The noise of the actually acquired CT images depicted as *thin lines*. *Thick lines* represent the noise in the simulated images

over the whole imaging range. The same trend was also observed in evaluations using a FOV of 400 mm. Evaluations using a FOV of 240 mm showed a small overestimation of noise in the shoulder and abdominal regions.

Box-and-whisker plots of all evaluated configurations are shown in Fig. 6 (tube voltage 120 kV; tube current 300/150/80/40/20 mA; FOV 400/320/240 mm). Mean differences in noise measurements between actual and simulated images were calculated for all configurations (dose level in combination with a FOV) over 290 slices (Table 2). Evaluations showed similar differences calculated per FOV, i.e. 3.5±2.1% for 400 mm; 3.1±1.9% for 320 mm; 3.2±3.5% for 240 mm. Mean differences per dose level also showed differences within 4%, i.e. 2.3±1.7% (300 mA), 3.5±2.2% (150 mA), 3.5±2.7% (80 mA), 3.7± 2.7% (40 mA), and 3.5±3.1% (20 mA).

Discussion

The study was aimed at evaluating a low dose simulation technique that can be applied to the raw data of CT
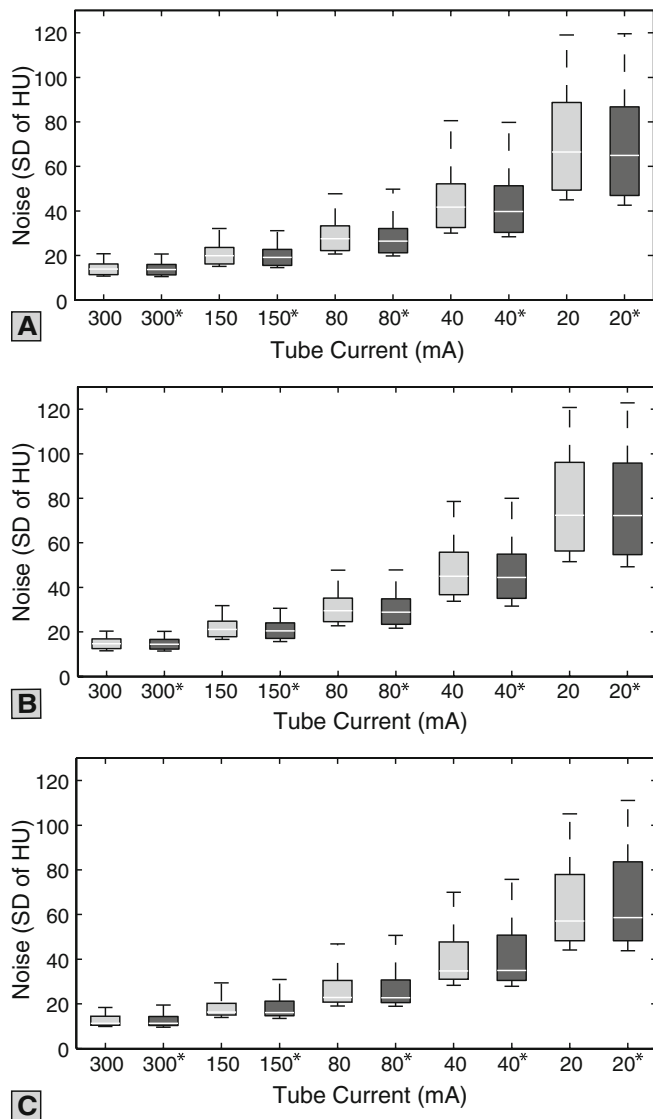
Fig. 6 Box plots of noise measurements in the anthropomorphic phantom. Simulations were performed from 500 mA downwards to 300, 150, 80, 40 and 20 mA. *Light boxes* correspond to actual and *dark boxes* (tube current with *asterisks*) correspond to simulated images. Three configurations are presented: 120 kV in combination with FOV 400 mm (**a**), FOV 320 mm (**b**) and FOV 240 mm (**c**)

acquisitions. Low dose simulations and actual acquired low dose images corresponded well for both the cylindrical test object and the anthropomorphic phantom. The mean difference in noise over all comparisons was 5.0% for the cylindrical test object and 3.3% for the anthropomorphic phantom. Also the noise power spectrum showed overall comparable shape and intensity, meaning that noise in actual and simulated lower dose images will affect visual appearance and diagnosis in a similar way. The major practical benefit of the algorithm is that it can be retrospectively applied to CT to optimise acquisition protocols in order to reduce the radiation dose. The software has become available for researchers to perform clinical studies in order to investigate the possibility of dose reduction for clinical CT protocols.

To illustrate the benefits of the algorithm, the results of a patient study are presented. Figure 7 shows a cardiac coronary CT angiogram (64-slice CT; Aquilion 64; tube voltage 120 kV, tube current 250 mA, pitch 0.197 and beam collimation 64×0.5 mm). The acquisition was simulated downwards to three dose levels, 50%, 25% and 12.5%. The curved multiplanar reconstructions (MPR) show the right coronary artery (RCA). As can be seen in the MPR, the CT revealed a significant stenosis in the RCA. Image quality of the coronary CT angiograms at low doses is obviously affected by noise; the influence of noise on the clinical diagnosis is now being studied in an observer study.

In the current implementation of the low dose CT simulator, calibration data have to be separately obtained for each combination of tube voltage and FOV. To evaluate the performance of another tube voltage, the same evaluations were also applied for tube voltage 135 kV in combination with three FOV. Because of a limitation in the generator of the CT, the simulations with this tube voltage were performed downwards starting at 400 mA instead of 500 mA. Mean difference in noise over all comparisons for tube voltage 135 kV between actual and simulated images was 4.1±4.0% for the cylindrical test object and 3.8±2.9% for the anthropomorphic phantom. These results implied comparable performance at other tube voltages.

Clinical studies aimed at optimising CT acquisition protocols with low dose simulators have already been performed by several groups for colonoscopy [6, 11], lung nodules [8], pulmonary angiography [10], acute appendi-

Table 2 Mean differences in noise between actual and simulated images of the anthropomorphic phantom calculated over all 290 slices

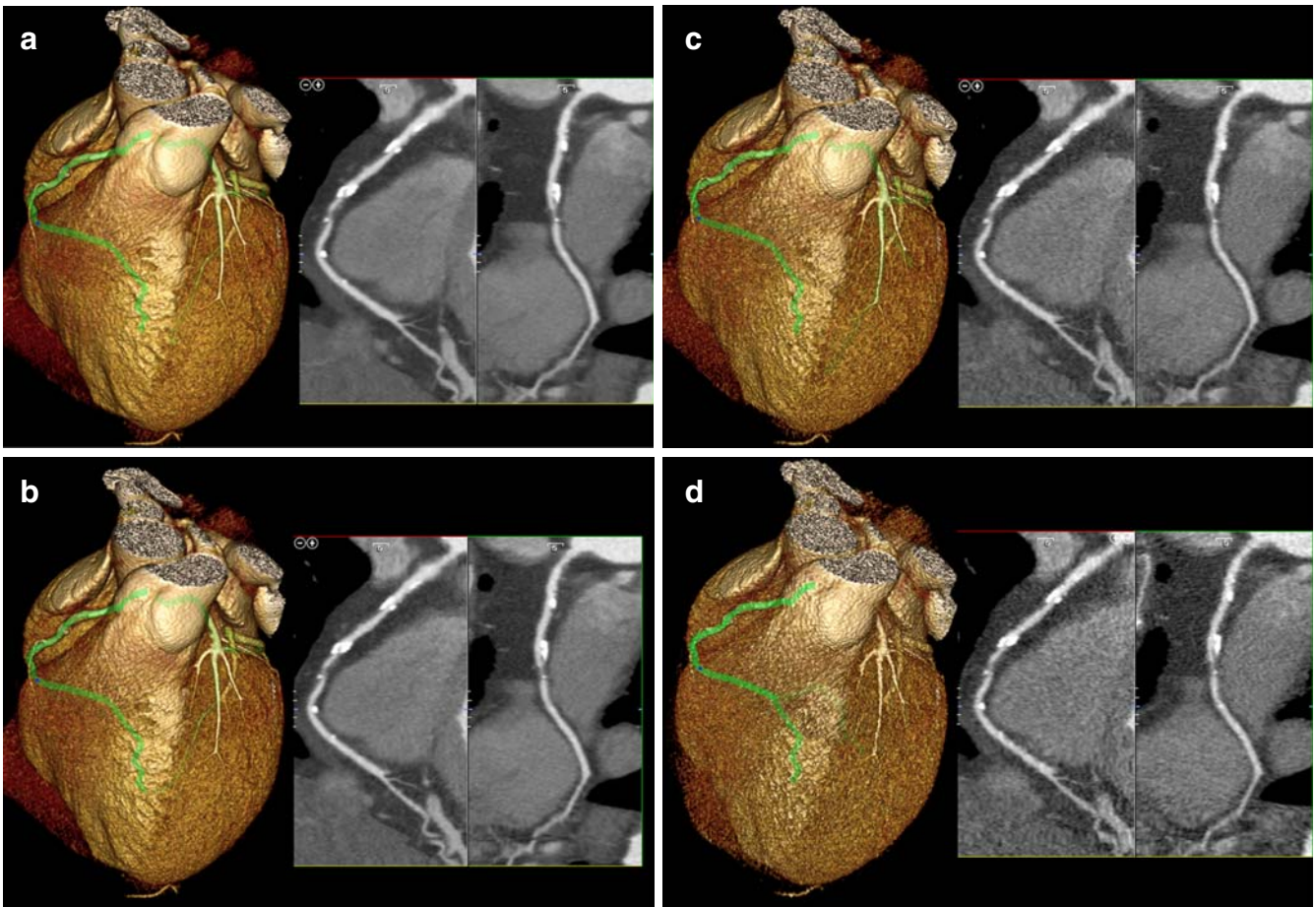|	Mean differences ± SD (%)				
	300 mA	150 mA	80 mA	40 mA	20 mA
120 kV–FOV 400 mm	1.96±1.30	3.50±1.63	3.75±1.46	4.40±2.43	3.82±2.39
120 kV–FOV 320 mm	2.44±1.52	4.06±1.74	3.49±2.09	3.03±1.93	2.52±1.73
120 kV–FOV 240 mm	2.42±2.18	2.94±2.92	3.13±3.82	3.60±3.41	4.03±4.41

Fig. 7 Clinical example of low dose simulations performed on 64-slice coronary CT angiography (male patient, aged 47 years). CT protocol: beam collimation 64×0.5 mm, tube voltage 120 kV, tube current 250 mA and helical pitch 0.197. The acquired image (**a**) was simulated downwards to 50% (**b**), 25% (**c**) and 12.5% (**d**). Curved multiplanar reconstructions were performed for the right coronary artery and show a significant stenosis

citis [14] and abdominal CT for paediatrics [7]. However, none of these low dose simulators has been thoroughly evaluated, e.g. with noise power spectrum assessment or noise measurements in an anthropomorphic phantom. These publications relate to three different low dose simulation algorithms which are performed on raw data and to one technique in which operations are performed on the reconstructed image data. This latter technique [14] has a major drawback as the noise of a uniform phantom is added to the clinical image, thus differences in radiation absorption of materials within the patient are not taken into account leading to unrealistic simulations.

Before starting clinical observer studies by means of low dose simulations on clinical data, one should always quantitatively verify the accuracy of the simulations. This study has shown that the described simulation method is applicable for dose levels down to 10 mAs (tube current 20 mA with rotation time 0.5 s). The differences between actual and simulated images were accurately determined to evaluate the correctness of the simulations. Overall differences in noise between actual and simulated images up to 10% are considered acceptable for clinical studies. This is supported by a recent study that has shown that just noticeable differences in noise levels are approximately 25%, i.e. a radiologist is only able to distinguish a difference in noise in excess of 25% [9].

There are several options to decrease the radiation dose, i.e. by increasing the pitch factor, decreasing the tube voltage or decreasing the tube current. However, the simulation methodology described in this paper only applies to dose reduction resulting from reduced tube current at a fixed pitch factor and tube voltage.

Comparisons at the lowest dose level in combination with FOV 240 mm showed greater differences between actual and simulated images in relation to other dose levels and FOVs. This dose level probably results in dominating detector noise. Accordingly, when detector noise becomes prominent, our low dose simulation method shows less accurate results.

Multiple strategies have been realised over the last few years for the optimisation of radiation dose, e.g. by using tube current

966

modulation. This technique is primarily used to improve the consistency of interpatient and intrapatient images. Low dose simulations are in these cases more complex to perform because the actual tube current and simulated tube current should individually be determined for each projection in the raw data. Currently this is being implemented in the low dose CT simulator and will be evaluated. Consequently, the software also has the potential to perform accurate simulations with modern acquisition techniques.

The low dose simulator method is applicable for every CT manufacturer. However CT manufacturers often disable users from editing raw CT data. For our software Toshiba Medical Systems provided access to the raw CT data and therefore the software is now dedicated to the Toshiba raw CT data format.

Conclusion

In this study the development and evaluation of a low dose simulator is described. The evaluations have shown good agreement with regard to noise, HU and NPS measurements. Differences that were found are acceptable for clinical studies. Our results have shown that the low dose simulator can be used to produce reliable lower dose images for clinical studies.

References

1. National Council on Radiation Protection and Measurements (NCRP) (2009) Report No 160. Ionizing radiation exposure of the population of the United States. NCRP, Bethesda
2. Brenner DJ, Hall EJ (2007) Computed tomography—an increasing source of radiation exposure. N Engl J Med 357:2277–2284
3. Mayo JR, Whittall KP, Leung AN, Hartman TE, Park CS, Primack SL, Chambers GK, Limkeman MK, Toth TL, Fox SH (1997) Simulated dose reduction in conventional chest CT: validation study. Radiology 202:453–457
4. Veldkamp WJ, Kroft LJ, van Delft JP, Geleijns J (2009) A technique for simulating the effect of dose reduction on image quality in digital chest radiography. J Digit Imaging 22:114–125
5. Britten AJ, Crotty M, Kiremidjian H, Grundy A, Adam EJ (2004) The addition of computer simulated noise to investigate radiation dose and image quality in images with spatial correlation of statistical noise: an example application to X-ray CT of the brain. Br J Radiol 77:323–328
6. Florie J, van Gelder RE, Schutter MP, van Randen A, Venema HW, de Jager S, van der Sluys Veer A, Prent A, Bipat S, Bossuyt PM, Baak LC, Stoker J (2007) Feasibility study of computed tomography colonography using limited bowel preparation at normal and low-dose levels study. Eur Radiol 17:3112–3122
7. Frush DP, Slack CC, Hollingsworth CL, Bisset GS, Donnelly LF, Hsieh J, Lavin-Wensell T, Mayo JR (2002) Computer-simulated radiation dose reduction for abdominal multidetector CT of pediatric patients. AJR Am J Roentgenol 179:1107–1113
8. Hanai K, Horiuchi T, Sekiguchi J, Muramatsu Y, Kakinuma R, Moriyama N, Tuchiiya R, Niki N (2006) Computer-simulation technique for low dose computed tomographic screening. J Comput Assist Tomogr 30:955–961
9. Massoumzadeh P, Don S, Hildebolt CF, Bae KT, Whiting BR (2009) Validation of CT dose-reduction simulation. Med Phys 36:174–189
10. Tack D, De M V, Petit W, Scillia P, Muller P, Suess C, Gevenois PA (2005) Multi-detector row CT pulmonary angiography: comparison of standard-dose and simulated low-dose techniques. Radiology 236:318–325
11. van Gelder RE, Venema HW, Serlie IW, Nio CY, Determann RM, Tipker CA, Vos FM, Glas AS, Bartelsman JF, Bossuyt PM, Lameris JS, Stoker J (2002) CT colonography at different radiation dose levels: feasibility of dose reduction. Radiology 224:25–33
12. Boedeker KL, Cooper VN, Nitt-Gray MF (2007) Application of the noise power spectrum in modern diagnostic MDCT: part I. Measurement of noise power spectra and noise equivalent quanta. Phys Med Biol 52:4027–4046
13. Shrimpton PC, Wall BF, Fisher ES (1981) The tissue-equivalence of the Alderson Rando anthropomorphic phantom for x-rays of diagnostic qualities. Phys Med Biol 26:133–139
14. Fefferman NR, Bomsztyk E, Yim AM, Rivera R, Amodio JB, Pinkney LP, Strubel NA, Noz ME, Rusinek H (2005) Appendicitis in children: low-dose CT with a phantom-based simulation technique—initial observations. Radiology 237:641–646